Optical-absorption studies of wurtzite-phase $Zn_{1-x}Mn_xSe$

J. E. Morales, W. M. Becker, B. I. Wang, and U. Debska
Department of Physics, Purdue University, West Lafayette, Indiana 47907

J. W. Richardson
Department of Chemistry, Purdue University, West Lafayette, Indiana 47907

(Received 5 August 1988; revised manuscript received 6 March 1989)

Optical-absorption results on single-crystal samples of $Zn_{1-x}Mn_xSe$ are presented. Dichroism associated with the fundamental edge is established for $x \geq 0.35$, consistent with the onset of the wurtzite phase. Up to four absorption bands associated with Mn^{2+} intraion transitions are seen at $x \sim 0.50$; the shifts of the three lowest transitions with x are analyzed with use of ligand-field theory applied to localized $MnSe_4$ clusters. Consistent polarization in the Mn absorption spectrum occurs in the wurtzite region. Possible mechanisms leading to such polarizations are considered.

I. INTRODUCTION

$Zn_{1-x}Mn_xSe$ is among a group of materials formed by alloying a II-VI compound semiconductor with a binary chalcogenide containing a magnetic ion. Such systems are designated dilute magnetic semiconductors (DMS's).[1] Growth of high-quality single crystals containing large molar fractions of the transition element manganese[2] has allowed rapid progress in this field, both for fundamental studies[3,4] and for novel device applications.[5] In these materials the Mn ion is isovalent with the cation, and is introduced substitutionally on the cation site: overall distribution among the sites is considered to be random. Interaction between the magnetic moments of the Mn^{2+} ions with band carriers occur via spin-spin exchange and other interactions. These interactions are strongly affected by external magnetic fields as seen in a variety of investigations of DMS's involving such fields, including giant-exciton Faraday rotation,[6] large g factors in $Hg_{1-x}Mn_xTe$,[7] and magnetic polaron effects in $Cd_{1-x}Mn_xTe$ (Refs. 8 and 9) and $Cd_{1-x}Mn_xSe$.[10]

Even with no external magnetic field, the presence of Mn may be strongly manifested in the optical properties of DMS's. For example, in $Zn_{1-x}Mn_xSe$ with $x \sim 0.001$ (band-gap energy $E_g \sim 2.8$ eV), three absorption bands associated with Mn^{2+} intraion transitions are seen below the intrinsic edge.[11] These have been identified (in increasing energy) with the ${}^6A_1({}^6S) \rightarrow {}^4T_1({}^4G)$, ${}^6A_1({}^6S) \rightarrow {}^4T_2({}^4G)$, and ${}^6A_1({}^6S) \rightarrow {}^4A_1, {}^4E({}^4G)$ transitions of Mn^{2+} in the $3d^5$ configuration. A review of the literature on DMS's reveals that a general increase in gap energy with Mn mole fraction x occurs at fixed temperature T, whereas the energies of the Mn transitions are relatively insensitive to x.[12] For $Zn_{1-x}Mn_xSe$ the upper limit of the region of solid solution is $x \sim 0.57$.[13] In samples with x approaching this value, the intrinsic edge shifts to $E_g \sim 3.1$ eV, and some of the higher Mn transitions corresponding to those seen in the wider-gap DMS $Zn_{1-x}Mn_xS$ (Ref. 14) become accessible.

The first work on solid solutions of $Zn_{1-x}Mn_xSe$ indicated that the material crystallizes in the zinc-blende structure for $x \leq 0.35$, and in the wurtzite structure for $0.35 \leq x \leq 0.50$.[15] As yet, little information is available in the literature on the dichroism associated with the intrinsic edge in the wurtzite region. Also, although the Mn^{2+} transitions are localized, polarization effects related to crystalline anisotropy in the same region may be anticipated. Recent availability of good-optical-quality samples for $0 \leq x \leq 0.5$ allows optical-absorption measurements at high x which address both problems. Absorption results related to these problems are reported below. Also included are data for $x < 0.3$ which establish the continuity of various effects, i.e., $E_g(x,T)$, and characteristics of the d-d transitions across the zinc-blende–wurtzite phase boundary.

A description of the experimental methods and equipment is given in Sec. II. The results are presented in Sec. III. We discuss various aspects of the results in Sec. IV.

II. EXPERIMENT

The crystals used in this study were grown by the modified Bridgman method.[2] We utilized samples taken from ingots of nominal compositions $x \sim 0.23$, ~ 0.35, and ~ 0.50. The samples with $x \sim 0.23$ were unoriented. Crystal orientations of the $x \sim 0.35$ and ~ 0.50 samples were made first by examination of characteristic cleavage patterns and then by x-ray technique. For each composition, samples of different thickness were required to cover the spectral region investigated. In these cases adjacent slices were cut from a given region of the ingot before initiating the thinning procedure. Comparisons of the energetic positions of the intrinsic edge at 10 K with E_g versus x values obtained by piezomodulated reflectivity at the same temperature[16] gives x values within ± 0.01 of the nominal values. Sample-preparation techniques and measurement procedures are identical to those described previously in our work on the $Cd_{1-x}Mn_xSe$ alloy system.[17] Use of a cold-finger cryostat limited the results to three fixed temperatures, 300 K [room temperature

 ©1989 The American Physical Society

(RT)], ~77 K [liquid-nitrogen temperature (LN_2)], and ~10 K [liquid-helium temperature (LHe)].

III. RESULTS

Figure 1 shows absorption spectra ranging from the Mn absorption threshold up to the intrinsic edge in an $x \sim 0.23$ sample. Absorption coefficients were calculated using the formula appropriate for multiple reflections at normal incidence for samples with parallel faces,

$$T = \frac{(1-R)^2 e^{-\alpha t}}{1-R^2 e^{-2\alpha t}} , \quad (1)$$

where T is the fraction of transmitted light I_T/I_0, t is the sample thickness, α is the absorption coefficient, and R is the sample reflectance.

The index of refraction in $Zn_{1-x}Mn_xSe$ alloys is not known as yet. For good matching between samples, the reflectance coefficient R in Eq. (1) was taken as that obtained by assuming zero absorption at maximum experimental transmission, usually at 7000 Å, in the appropriate thin sample. R values of the order ~0.3 (see Table I) were used to bring the LHe data for samples 1 and 2 into coincidence near the Mn threshold.

Figure 2 gives absorption spectra ranging from the Mn absorption threshold up to the intrinsic edge in a thin ~0.35 sample for E||c. Somewhat similar results (not shown) are obtained for E⊥c on the same sample. Details near the intrinsic edge are revealed in Fig. 3, where results are plotted for both orientations of the electric field E. Consistency relating to band-edge dichroism was obtained only after extreme care was exercised in strain-free mounting. Extension of the data below the Mn absorption threshold at LHe is seen in Fig. 4 using a thicker sample. Two reflectances are employed (see Table I), one for each polarization, in the overlap region near the Mn threshold. Differences in R with the direction of the field E appear to be systematic. The reduced values of R required for sample 4 are of uncertain origin (they may possibly be due to differences in etching procedures); their use does not, however, appear to alter the general features of the spectra in Fig. 4 for $h\nu > 2.4$ eV.

TABLE I. Reflectances for various samples (at 7000 Å and LHe temperature).

Sample no.	x	t (μm)	R(E||c)	R(E⊥c)
1	~0.23	25		0.279
2	~0.23	926		0.329
3	~0.35	13.2	0.332	0.335
4	~0.35	690	0.202	0.209
5	~0.50	7.8	0.284	0.315
6	~0.50	502	0.284, 0.310	0.315

Figure 5 gives absorption spectra ranging from the Mn absorption threshold up to the intrinsic edge in a thin $x \sim 0.50$ sample for E||c in the same sample. In Fig. 6 we give details near the intrinsic edge for both orientations of the field E. Figure 7 extends the LHe data below the Mn absorption threshold using a thick sample.

Figure 1 shows the general behavior expected for the $Zn_{1-x}Mn_xSe$ alloy system. We find (1) a sharp rise of the

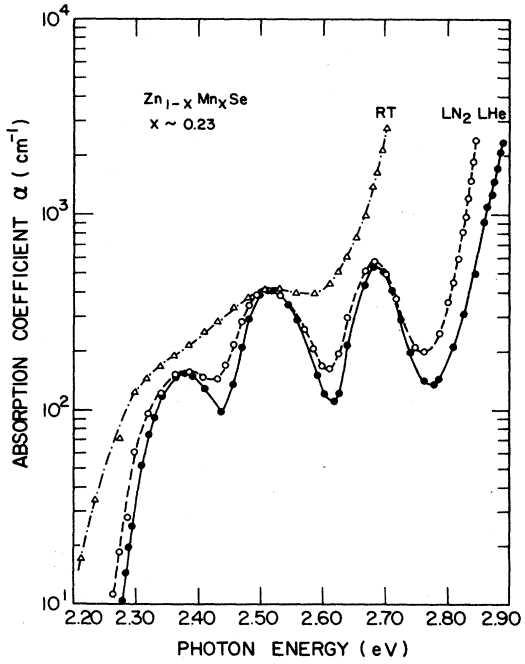

FIG. 1. Optical-absorption coefficient vs photon energy in $x \sim 0.23$ sample 1.

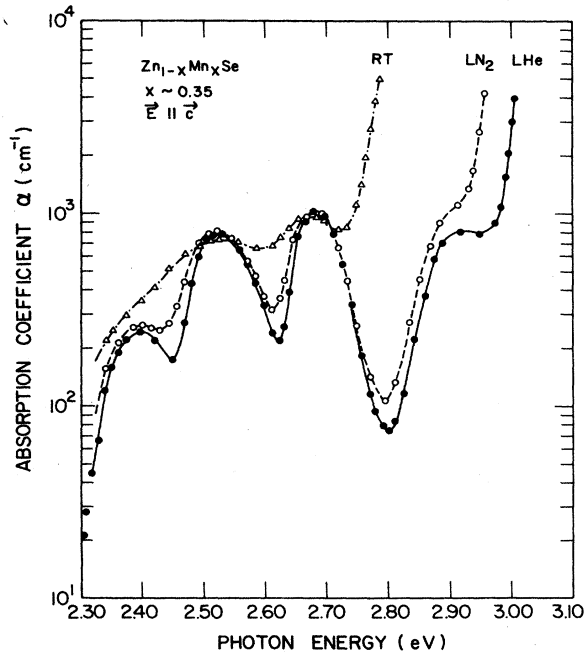

FIG. 2. Optical-absorption coefficient vs photon energy for E||c in $x \sim 0.35$ sample 3.

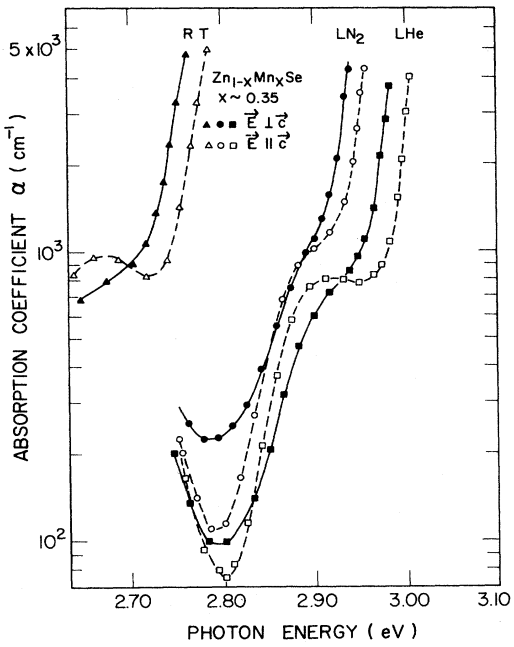

FIG. 3. Optical-absorption coefficient vs photon energy in $x \sim 0.35$ sample 3.

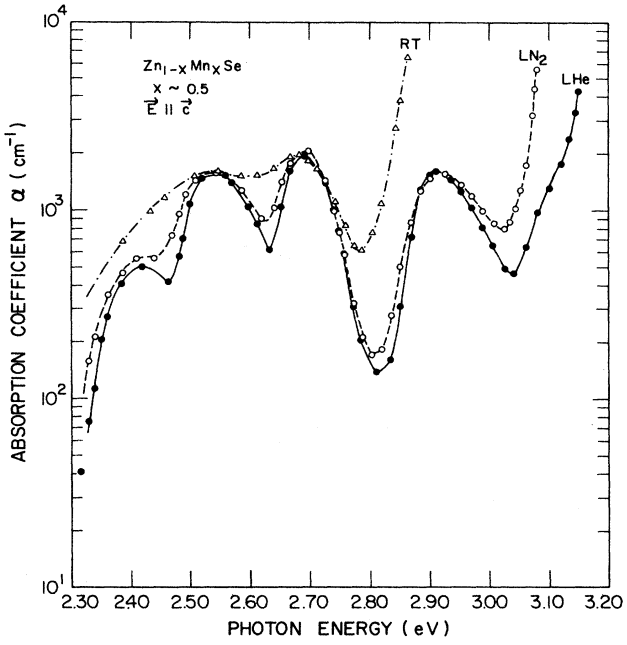

FIG. 5. Optical-absorption coefficient vs photon energy for $\mathbf{E} \| \mathbf{c}$ in $x \sim 0.50$ sample 5.

absorption, exceeding $\sim 10^3$ cm^{-1}, and indicating a direct band-to-band transition, (2) a shift of this absorption edge to higher energy with decreasing temperature, and (3) emergence of distinct maxima and minima associated with Mn^{2+} intraion transitions with lowered temperature. Figure 2 reveals behavior similar to Fig. 1. In addition to the three maxima seen in the $x \sim 0.23$ sample, a distinct shoulder appears near the band edge, presaging the emergence of a fourth maximum. The revealing of

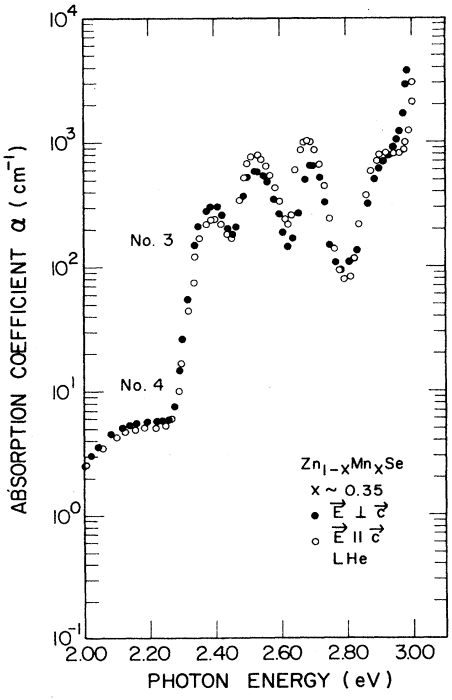

FIG. 4. Optical-absorption coefficient vs photon energy in $x \sim 0.35$ samples 3 and 4.

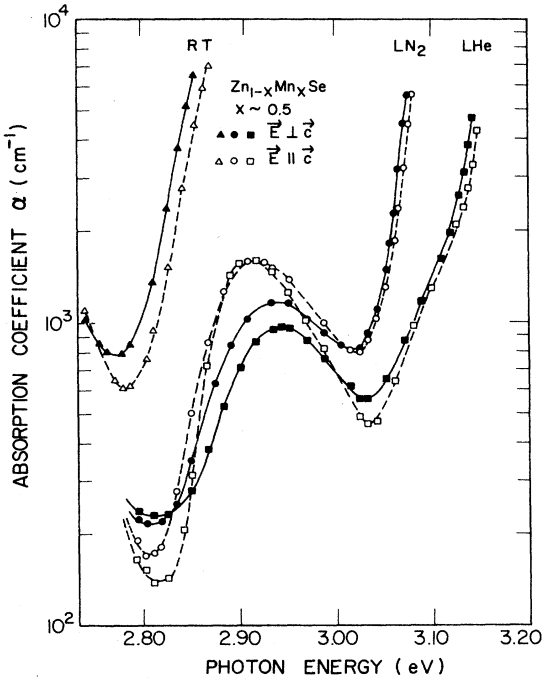

FIG. 6. Optical-absorption coefficient vs photon energy in $x \sim 0.50$ sample 5.

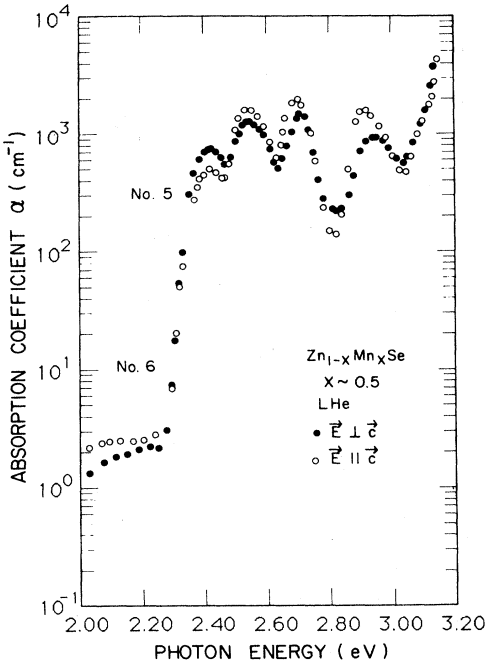

FIG. 7. Optical-absorption coefficient vs photon energy in $x \sim 0.50$ samples 5 and 6.

this shoulder and its evolution into a maximum, as seen in Figs. 5 and 6, follows from the compositional dependence of the band gap. Positions of various maxima and their identifications are listed in Table II.

No polarization features are expected for samples 1 and 2, since they have the zinc-blende structure. The dichroism associated with the band edge in Figs. 3 and 6 is attributed to the valence-band splitting expected for the wurtzite structure. The values of this splitting, Δ, given in Table III, are taken at constant α's. Estimates of rates of energy shift with temperature, all obtained for α's well in excess of manganese absorption contributions, are listed in Table IV.

Polarization features in the manganese absorption region appear to be consistent between the thin $x \sim 0.35$ and ~ 0.50 samples. For the lowest-energy transition (at ~ 2.4 eV), $\alpha(\mathbf{E}\perp\mathbf{c}) > \alpha(\mathbf{E}\|\mathbf{c})$, while at the two next-higher transitions (at ~ 2.53 and ~ 2.7 eV), $\alpha(\mathbf{E}\|\mathbf{c}) > \alpha(\mathbf{E}\perp\mathbf{c})$. Furthermore, at ~ 2.7 eV there is a small energy separation of the maxima for the two polarizations. A similar separation is observed in the $x \sim 0.5$ sample for the maxima at ~ 2.9 eV (see Table II). Consistency of polarization behavior regarding minima in both samples is also to be noted. The validity of the results was checked by independent measurements[18] on an $x \sim 0.35$ sample with the c axis perpendicular to the polished surfaces. For orthogonal directions with $\mathbf{E}\perp\mathbf{c}$, the positions and magnitudes of the absorption maxima were found to be independent of the direction of E. As in $Cd_{1-x}Mn_xSe$,[17] there is absence of dichroism at the Mn absorption threshold (~ 2.3 eV). Piezomodulated-reflectivity results on $Zn_{1-x}Mn_xSe$ which rely essentially on a volume-absorption affect near the same threshold also fail to reveal dichroic effects.[16]

A sharp break in absorption occurs near 2.3 eV in all the thick samples at LHe: a red shift and broadening of the Mn absorption edge is detected at higher temperatures (see Fig. 1), consistent with the data of Lee *et al.*[16]

IV. DISCUSSION

A. Absorption-edge dichroism

Samples in the wurtzite region exhibit the dichroism expected at the intrinsic edge, namely $\alpha(\mathbf{E}\perp\mathbf{c}) > \alpha(\mathbf{E}\|\mathbf{c})$. Band-edge dichrosim is explained in terms of a model first proposed by Birman.[19] In this model, the valence-band states of the wurtzite structure are derived from the Γ_{15} zinc-blende valence-band state through the action of two perturbations, spin-orbit coupling and crystal-field splitting. Transitions from the Γ_{9v} top valence band to the Γ_{7c} conduction band are allowed only for $\mathbf{E}\perp\mathbf{c}$. Transitions from the deeper crystal-field-split and spin-orbit-split Γ_{7v} valence band to the Γ_{7c} conduction band are allowed for both directions of polarization.

The smaller Γ_{9v}-Γ_{7v} valence-band splitting, designated Δ in the literature, and usually obtained from $E_{ex}(B) - E_{ex}(A)$, was found by Liang and Yoffee[20] to be ~ 65 meV in wurtzite-phase ZnSe grown by vapor transport. The results listed in Table III suggest a monotonic decrease in Δ with x in $Zn_{1-x}Mn_xSe$, behavior already noted by Stankiewicz in $Cd_{1-x}Mn_xSe$.[21] Taking $\Delta = 65$ meV as the $x = 0$ endpoint, we find $(d\Delta/dx)_{LHe} = 0.12 \pm 0.007$ eV for $Zn_{1-x}Mn_xSe$. A much weaker dependence on x, $d\Delta/dx \sim 0.031$ eV, is seen in $Cd_{1-x}Mn_xSe$ using the Stankiewicz data.[21] Both results

TABLE II. Position of absorption maxima (in eV) of Mn bands in $Zn_{1-x}Mn_xSe$ at LHe temperature.

Sample no.	x	t (μm)	Polariz.	$^4T_1(^4G)$	$^4T_2(^4G)$	$^4A_1{}^4E(^4G)$	Other
	0.001[a]			2.34	2.48	2.655	
1	0.23	25		2.380	2.510	2.680	
3	0.35	13.2	∥	2.393	2.522	2.684	~2.9
3	0.35	13.2	⊥	2.396	2.532	2.697	
5	0.50	7.8	∥	2.420	2.535	2.695	2.913
5	0.50	7.8	⊥	2.420	2.545	2.707	2.94

[a]Reference 14.

TABLE III. Crystal-field splitting Δ for $Zn_{1-x}Mn_xSe$.

Sample no.	x	α (cm^{-1})	Δ (meV) 300 K	77 K	10 K
3	0.35	4000	21.7	17.2	20.7
5	0.50	4000	11.7	4.7	8.3
ZnSe[a]					65
$Zn_{1-x}Mn_xSe$[b]	0.39				20
	0.44				20
	0.57				14

[a]Reference 19.
[b]Reference 23.

imply disappearance of the Γ_{9v}-Γ_{7v} splitting in a hypothetical wurtzite MnSe structure.

As in our work on $Cd_{1-x}Mn_xSe$,[17] we find a "retrograde" thermal behavior of Δ, namely an increase in value from LN_2 to LHe temperature. Lee[22] has also observed this behavior in piezomodulated-reflectivity data on $x=0.35$ and 0.45 samples of $Zn_{1-x}Mn_xSe$; Stankiewicz and Fermin[23] find, however, nearly equal values of Δ at 8 and 77 K in an $x=0.44$ sample of $Zn_{1-x}Mn_xSe$, and an increased Δ at intermediate temperatures, using wavelength-modulation reflectivity. A number of possible mechanisms leading to temperature variations of Δ were discussed earlier,[17] as follows: (1) thermal-expansion effects equivalent to nonhydrostatic strains, (2) polaronic effects, (3) unrecognized contributions to the band-edge absorption due to overlapping Mn absorptions, and (4) the existence of multiphase inclusions, polytypism, or twinning at a microscopic level. With respect to (4), polytypism and twinning are characteristic of the $Zn_{1-x}Mn_xSe$ system,[3] but only for $0.2 \leq x \leq 0.3$, and mixed phases are expected only for $x > 0.57$.[13] The other mechanisms listed also seem unlikely, for reasons given in Ref. 17. Further work on this question is needed, considering the contradictory results among different investigators.

The behavior of the energy gaps of various semiconductors has been fitted by Varshni[24] using the empirical equation

$$E_g(T)=E_0-\frac{AT^2}{T+B} . \quad (2)$$

According to Eq. (2), linear behavior should be observed at high temperatures, but should merge smoothly toward saturation at low temperatures. The experiments of Diouri *et al.* on $Cd_{1-x}Mn_xTe$ (Ref. 25) suggested a departure from this behavior in other DMS's at high x: when cooling from room temperature, E_g approaches a plateau around LN_2, but then undergoes a "blueshift" and a second region of saturation well above the value predicted from the high-temperature data, upon further cooling. Existence of this effect has been inferred in $Zn_{1-x}Mn_xTe$ (Ref. 26) and $Cd_{1-x}Mn_xSe$ (Ref. 17) from optical-absorption results at fixed temperatures (RT, LN_2, and LHe), and has been more directly seen in $Zn_{1-x}Mn_xSe$ at high x using band-edge photoluminescence[3] and wavelength-modulated reflectivity.[23] The observed shifts appear to be related to *s-d* and *p-d* interactions. Reviewing the results given in Table IV, the $x \sim 0.23$ and ~ 0.35 sample behaviors are consistent with Eq. (2); the $x \sim 0.5$ sample deviates from this behavior—only slightly for $\mathbf{E} \perp \mathbf{c}$ and somewhat more significantly for $\mathbf{E} \| \mathbf{c}$. Inspection of Fig. 4 in Ref. 4 and the data of Stankiewicz and Fermin[23] suggests that these separate results are compatible, based on the observed "blue" shifts, namely that these shifts are insufficient to be reflected in the $10 \leq T \leq 77$ K averages listed in Table III.

B. Manganese absorption

The three lowest absorption bands listed in Table II closely correspond in energies and spacings to the three

TABLE IV. Averaged temperature coefficients.

Sample no.	x	α (cm^{-1})	Polarization	$\overline{-dE_g/dT}$ (10^{-4} eV/K) $77<T<300$ K	$10<T<77$ K
1	0.23	2000		6.73	5.98
3	0.35	4000	∥	7.87	7.49
3	0.35	4000	⊥	8.08	6.97
5	0.50	4000	∥	9.97	11.00
5	0.50	4000	⊥	10.28	10.48
	0.066[a]			4.7	
	0.36[a]			8.5	
	0.55[a]			9.7	

[a]Reference 3.

lowest Mn-associated transitions seen by Langer and Richter.[11] From these, we derive values of the Racah parameters B and C, and the crystal-field parameter Dq ($=-\frac{9}{40}$ the difference between energies of the de and dt_2 orbitals), using the Tanabe-Sugano energy matrices[27,28] and the experimental values of the maxima listed in Table II. The method involves a Taylor-series expansion[29] of the 3×3 $[Dq,B,C,E(^4T_1)]$ and 3×3 $[Dq,B,C,E(^4T_2)]$ secular equations, and use of the 2×2 $[B,C,E(^4A_1,{}^4E)]$ secular equation. Assuming $C/B=3.7$ and performing a least-squares fit, we obtain for $x\sim0.50$, $B=752$ cm^{-1}, $C=2782$ cm^{-1}, and $Dq=353$ cm^{-1}; for $x\sim0.35$, $B=749$ cm^{-1}, $C=2772$ cm^{-1}, and $Dq=369$ cm^{-1}. Finally, for $x\sim0.23$, we find $B=750$ cm^{-1}, $C=2760$ cm^{-1}, and $Dq=372$ cm^{-1}. A fourth band is also seen for $x\geq0.35$; it probably is the transition to $^4T_2(^4D)$ or $^4T_1(^4P)$.

Ves *et al.*[30] assign two absorption bands appearing above the $^6A_1(^6S)\rightarrow{}^4A_1,{}^4E(^4G)$ transition to the $3d^5$ configuration of Mn^{2+}, based on the pressure-induced red shifts observed. Extrapolation of their data to $P=0$ suggests that the lower of their two bands corresponds to the ~2.93-eV absorption band seen in our $x\sim0.50$ sample at LHe. Less certain is the correspondence between the ~3.10-eV shoulder seen by us and the higher-energy feature observed by Ves *et al.*[30] in an $x=0.25$ sample at pressures just below the phase transition.

C. Polarization and x dependence of Mn transitions

While the basic features of the spectra ascribed to Mn^{2+} d-d transitions are well characterized, the more subtle aspects of their polarization and small x dependence are not readily understood. Here we investigate whether certain other known structural features do or do not explain these observations.

1. Bulk effects due to wurtzite structure

Polarization effects in the Mn absorption spectra cannot be explained by ligand-field theory applied to the localized $MnSe_4$ clusters, since they retain near-T_d symmetry even in the wurtzite phase. It is therefore logical to consider the possible influence of the farther contributions to the crystal field, generated by ions external to the cluster and having C_{3v} symmetry in the wurtzite phase. Energetic effects on the d-d transitions from the field of these external ions are usually considered weak.[31,32] Their contribution to the polarization effects cannot immediately be ruled out, however.

Under a C_{3v} perturbation and neglecting spin-orbit coupling, symmetries of the $^6A_1$ ground and the nearly degenerate ^4E and $^4A_1$ excited levels of the $MnSe_4$ cluster are unchanged, but the $^4T_1$ and $^4T_2$ excited levels are split into $^4E+{}^4A_2$ and $^4E+{}^4A_1$, respectively (see right side of Fig. 8). Excluding phonon-assistance and spin effects, only $E\leftrightarrow A_1$ and $A_1\leftrightarrow A_1$ transitions are electric dipole allowed, with polarizations $\mathbf{E}\perp\mathbf{c}$ and $\mathbf{E}\|\mathbf{c}$, respectively. Furthermore, according to the calculation of Parrot *et al.*,[33] in T_d symmetry the $^4A_1\leftrightarrow{}^6A_1$ transition, while allowed, has 10^{-3} times the intensity of the

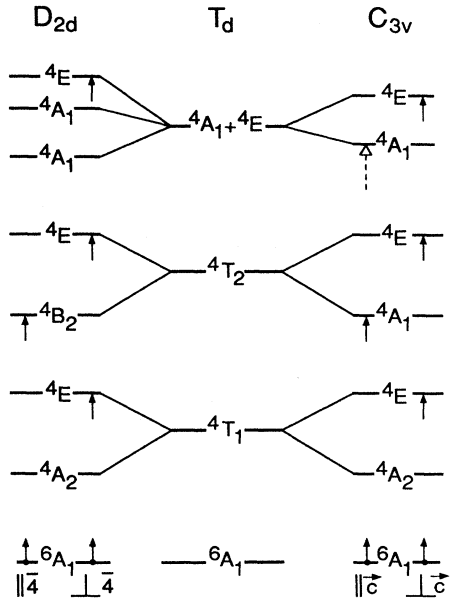

FIG. 8. Effects of symmetry reduction on T_d Mn d-d energy levels and resulting selection rules, indicated by arrows. C_{3v} results from inclusion of bulk effects in wurtzite phase and D_{2d} from the particular local distortion shown in Fig. 9. Polarizations are relative to the wurtzite c axis and to the $\bar{4}$ axis of the distorted central $MnSe_4$ unit of Fig. 9, respectively.

$^4E\leftrightarrow{}^6A_1$ transition. Thus the former is not even identified in spectra of the cubic phase. If similar behavior persists in the wurtzite phase, the absorption coefficient for $\mathbf{E}\|\mathbf{c}$ $[^6A_1\rightarrow{}^4A_1(^4A_1)]$ should at most be much weaker than for $\mathbf{E}\perp\mathbf{c}$ $[^6A_1\rightarrow{}^4E(^4E)]$.

The experimental spectra show three bands of similar intensities, displaced by just ~0.01 eV (Table II) for the two polarizations. In contrast, these elementary predictions lead to only one observable band for $\mathbf{E}\|\mathbf{c}$, namely $^6A_1\rightarrow{}^4A_1(^4T_2)$. Therefore, the long-range reduced C_{3v}-site symmetry of the wurtzite phase accounts for neither the similarities between polarized components nor the x dependence of transition energies.

2. Phonon effects

Another possible parallel explanation is that different types of phonons are involved in the perpendicular and parallel transitions, giving rise to different absorptions. This effect is difficult to establish experimentally because of absence of any detailed phonon structure. Also, on the other hand, phonon interaction would be expected to weaken the C_{3v} selection rules and lead to some depolarization.

3. Microscopic structural distortions

Yoder-Short *et al.*[13] have shown that Vegard's law is obeyed in $Zn_{1-x}Mn_xSe$. (Here, Vegard behavior is understood to include uniform scaling of all distances, random occupation of cation sites, and preservation of local

ionic-site symmetry, in the spirit of the virtual-crystal approximation.) The mean cation-cation distance increases linearly with x, continuity being preserved through the zinc-blende–to–wurtzite phase transition. Since the Mn-Se distance also would increase with x (although at a geometrically reduced rate), paralleling changes in Dq and consequent shift of the d-d absorption maxima in the $MnSe_4$ cluster would appear reasonable. This simple Vegard model, however, does not produce dichroism, since the local site symmetry remains T_d. Furthermore, it is inconsistent with more recent structural data.

Bunker *et al.*[34] obtained extended x-ray-absorption fine-structure (EXAFS) data on $Zn_{1-x}Mn_xSe$ and interpreted it according to the model of Balzarotti *et al.*[35] Using this model, they found nearly constant Mn—Se and Zn—Se bond lengths, equal to those observed in pure ZnSe and the hypothetical ($x=1$) wurtzite MnSe, throughout the $0<x<0.57$ alloy region. (Note that this interpretation eliminates no significant x dependence for the ligand-field Dq parameter.)

To a first approximation in the Balzarotti model, it is assumed that the cation sublattice of random Mn and Zn ions follows Vegard's-law behavior. Anion positions are then shifted to conform to (nearly) constant Zn-Se and Mn-Se bond lengths. As a result, the site symmetry of each Se is reduced from T_d, depending on the relative numbers and positions of its Zn and Mn nearest neighbors. Furthermore, such deformation attends *each* of the four Se ions of any given $MnSe_4$ cluster; thus, for larger values of x, most of these clusters also suffer distortion from T_d to a wide variety of lower symmetries.

To examine the perturbative effect of the Balzarotti-type model on the d-d excitations of the Mn^{2+} center first requires geometric analysis of the $2^{12}=4096$ possible "superclusters" ($MnSe_4Zn_{12-y}Mn_y$, $y=0,1,\ldots,12$), defined as a particular central $MnSe_4$ units plus its 12 adjacent cation neighbors (for one example with $y=5$, see Fig. 9). With the Mn-Se bond distance assumed constant, each particular configuration of the $12-y$ Zn ions thus produces a particular *bending* deformation of the $MnSe_4$ unit from T_d symmetry. Each of these deformations will, in general, split degeneracies of the electronically excited states in a particular way.

The deformation within the central $MnSe_4$ portion of each particular supercluster may be expressed as a linear combination of normal coordinates for bending modes of the tetrahedral unit, $Q(\Gamma\gamma)$, where $\Gamma\gamma = e\theta, e\varepsilon; t_2\xi, t_2\eta, t_2\zeta$. R_x, R_y, R_z are subspecies of irreducible representations of the T_d group. Likewise, the deformation perturbation V added to the Hamiltonian of the undistorted $MnSe_4$ cluster in each supercluster, may be represented as a linear combination of terms $V(\Gamma\gamma)$. This form of the perturbation V is identical to that used in analysis of the Jahn-Teller (JT) effect and we may draw upon it to assess the consequence of each deformation on the d-d spectrum.

The following simplifying assumptions are made in deducing the preliminary results given below.

(a) The nonzero displacements of Se ions in all superclusters have the same magnitude, δ.

(b) Pure rotations of the $MnSe_4$ unit have no effect on the transition energies. As in the JT effect, the t_2 modes have much smaller spectral effects than the e modes. Only the latter are considered.

(c) Relative probabilities of occurrence of each supercluster are calculated as a function of x, using the postulates of Balzarotti *et al.*[35]

Carrying through the analysis with these assumptions shows that each of the d-d transitions becomes a manifold of 4096 *sets* of transitions, one set per supercluster. Each set consists of transitions to the individual components of that degenerate level (i.e., $^4T_1$, $^4T_2$, or ^4E), as split in energy according to the perturbation V created by the supercluster associated with that set. The degree of splitting is determined by U_e (the e-mode JT coupling parameter), δ, and the particular amount of e-mode character in the distortion of the central $MnSe_4$. The relative contribution of each set is fixed by the probability that the associated supercluster occurs at a given x.

Assuming the wurtzite structure, it results that each d-d transition becomes a band whose full width at half maximum averages $3U_e\delta$, which should be ≈ 0.06 eV and is comparable to widths observed. While the *average* transition energy for each manifold remains at the unperturbed value, the calculated ^4T bands are asymmetric. Even with the Mn-Se distance assumed fixed, the positions of the ^{4}T maxima do show a small variation with x, although at $\frac{1}{10}$ the observed rate. Because of the assump-

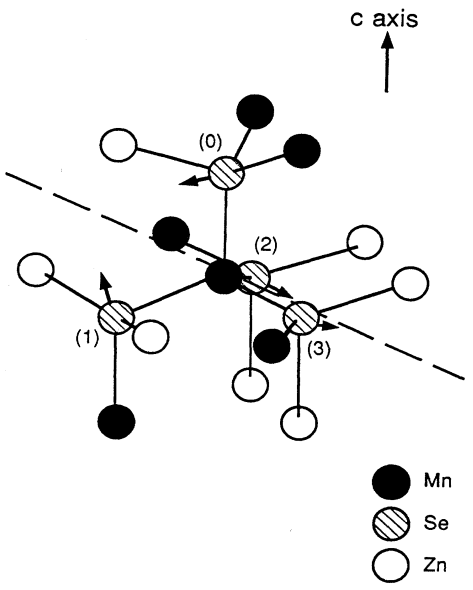

FIG. 9. Example of "supercluster" in wurtzite phase: for $y=5$, this produces a pure D_{2d} distortion of the central $MnSe_4$ unit, which is described by the normal mode $Q(e\theta)$ indicated by the Mn—Se bond rotations (arrows) shown. Rotations δ for Se ions (0) and (1) occur in the plane determined by them and the central Mn ion; rotations δ for Se ions (2) and (3) occur in the plane determined by them and the central Mn ion. The dotted line is the $\bar{4}$ axis of the distorted tetrahedron.

tions made, however, any given supercluster belongs to an ensemble with other equally probable, but essentially randomly oriented, superclusters. Consequently, *no* polarization is produced in any band, even in the C_{3v} wurtzite phase.

In other words, one significant feature of the Balzarotti-type model for local structure about each Mn ion is that in contrast to the model in subsection 1, it correctly predicts the three main spectral transitions to occur equivalently in *both* directions of polarization. Other interactions, however, evidently must be invoked to explain the displacements of the polarized maxima with respect to energy and x.

V. SUMMARY

We have studied optical-absorption effects in the region of the zinc-blende–wurtzite phase transition in $Zn_{1-x}Mn_xSe$. The dichroism associated with the fundamental edge is clearly established in the wurtzite region. Variations of E_g with x and T are in agreement with behavior found in other DMS wide-gap systems. Appreciable polarization features of Mn^{2+} intraion transitions are seen at high x. Several models taking into account reduction of symmetry of the crystal field from T_d were explored to explain the polatization effects. A detailed calculation is described which involves a distribution of bond angles surrounding the Mn ion. The analysis utilizes a model of "superclusters": it is shown that the polarization inherent in any given supercluster configuration will not be detectable for a random distribution of ions, and leads instead to depolarization. Other interactions therefore need to be considered to explain the current results.

ACKNOWLEDGMENTS

The authors wish to thank Professor S. Rodriquez for critical discussions relating to polarization effects. This work was supported in part by the U.S. National Science Foundation (Materials Research Group Program) Grant No. 85-20866.

[1]J. K. Furdyna, J. Appl. Phys. **53**, 7637 (1982); N. B. Brandt and V. V. Moshchkalkov, Adv. Phys. **33**, 193 (1984).
[2]U. Debska, W. Giriat, H. R. Harrison, and D. R. Yoder-Short, J. Cryst. Growth **70**, 399 (1984).
[3]R. B. Bylsma, W. M. Becker, J. Kossut, and U. Debska, Phys. Rev. B **33**, 8207 (1986).
[4]A. Twardowski, M. von Ortenberg, M. Demianiuk, and R. Pauthenet, Solid State Commun. **51**, 849 (1984).
[5]L. A. Kolodziejski, R. L. Gunshor, N. Otsuka, S. Datta, W. M. Becker, and A. V. Nurmikko, IEEE J. Quantum Electron. **QE-22**, 1666 (1986).
[6]J. A. Gaj, R. R. Galazka, and M. Nawrocki, Solid State Commun. **25**, 193 (1978).
[7]M. Jaczynski, J. Kossut, and R. R. Galazka, Phys. Status Solidi B **88**, 73 (1978).
[8]A. Golnik, J. A. Gaj, M. Nawrocki, R. Planel, and C. Benoit à la Guillaume, in Proceedings of the 15th International Conference on the Physics of Semiconductors, Kyoto, 1980 [J. Phys. Soc. Jpn. Suppl. A **49**, 819 (1980)].
[9]T. H. Nhung and R. Planel, Physica B+C **117&118B**, 488 (1983).
[10]M. Nawrocki, R. Planel, G. Fishman, and R. R. Galazka, Phys. Rev. Lett. **46**, 735 (1981).
[11]D. Langer and H. J. Richter, Phys. Rev. **146**, 554 (1966).
[12]W. M. Becker, in *Semiconductors and Semimetals,* edited by J. K. Furdyna and J. Kossut (Academic, New York, 1988), Vol. 25.
[13]D. R. Yoder-Short, U. Debska, and J. K. Furdyna, J. Appl. Phys. **58**, 4056 (1985).
[14]D. Langer and S. Ibuki, Phys. Rev. **138**, A 809 (1965).
[15]A. Pajaczkowska, Prog. Cryst. Growth Charact. **1**, 189 (1978).
[16]Y. R. Lee, A. K. Ramdas, and R. L. Aggarwal, Phys. Rev. B **38**, 10 600 (1988).
[17]J. E. Morales, W. M. Becker, and U. Debska, Phys. Rev. B **32**, 5202 (1985).
[18]J. F. MacKay (private communication).
[19]J. L. Birman, Phys. Rev. **115**, 1493 (1959).
[20]W. Y. Liang and A. D. Yoffe, Proc. R. Soc. London, Ser. A **300**, 326 (1967).
[21]J. Stankiewicz, Phys. Rev. B **27**, 3631 (1983).
[22]Y. R. Lee (private communication).
[23]J. Stankiewicz and José R. Fermín, J. Appl. Phys. **63**, 3300 (1988).
[24]Y. P. Varshni, Physica **34**, 149 (1967).
[25]J. Diouri, J. P. Lascaray, and M. El Amrani, Phys. Rev. B **31**, 7795 (1985).
[26]J. E. Morales Toro, W. M. Becker, B. I. Wang, U. Debska, and J. W. Richardson, Solid State Commun. **52**, 41 (1984).
[27]Y. Tanabe and S. Sugano, J. Phys. Soc. Jpn. **9**, 753 (1954).
[28]D. S. McClure, in *Solid State Physics,* edited by H. Ehrenreich, F. Seitz, and D. Turnbull (Academic, New York, 1959), Vol. 9.
[29]L. Pueyo, M. Bermejo, and J. W. Richardson, J. Solid State Chem. **31**, 217 (1980).
[30]S. Ves, K. Strössner, W. Gebhardt, and M. Cardona, Solid State Commun. **57**, 335 (1986).
[31]J. W. Richardson and G. J. M. Janssen, Phys. Rev. B **39**, 4958 (1989). See Table IX, in particular.
[32]The total potential field added to MnS_4^{6-} in zinc-blende $ZnS:Mn^{2+}$ shifts these transitions by less than 0.04 eV (see Ref. 31).
[33]R. Parrot and C. Blanchard, Phys. Rev. B **6**, 3992 (1972).
[34]B. A. Bunker, W.-F. Pong, U. Debska, D. R. Yoder-Short, and J. K. Furdyna, in *Diluted Magnetic (Semimagnetic) Semiconductors,* Vol. 89 of *Materials Research Society Symposia Proceedings,* edited by R. L. Aggarwal, J. K. Furdyna, and S. von Molnar (MRS, Pittsburgh, 1987), p. 231.
[35]A. Balzarotti, M. Czyżyk, A. Kisiel, N. Motta, M. Podgorny, and M. Zimnal-Starnawska, Phys. Rev. B **30**, 2295 (1984). This model has recently undergone further refinement based on thermodynamic arguments. See, for example, M. T. Czyżyk, M. Podgorny, A. Balzarotti, P. Letardi, N. Motta, A. Kisiel, and M. Zimnal-Starnawska, J. Phys. B **62**, 153 (1986).